BROKEN BAR DETECTION IN INDUCTION MOTORS
Using non intrusive torque estimation techniques

Eltabach Mario

Université Saint-Esprit de Kaslik, USEK Faculté des sciences et de génie informatique ; BP446 Jounieh, Liban

Charara Ali

HEUDIASYC UMR 6599; Université de Technologie de Compiègne BP 20529, 60205 Compiègne; Compiègne, France

Keywords: Diagnosis, control, supervision systems, Observers, signature analysis, Induction motors.

Abstract: One of the most important issues when implementing control and fault diagnosis systems for induction motor drives is obtaining accurate information about the state of certain motor electromagnetic signals such as stator flux and electromagnetic torque. This paper examines the detection of rotor imperfections through spectral analysis of the electromagnetic torque, computed by three stator flux estimators, and using only non-invasive sensors such as current and voltage sensors. The variable structure observer, the extended Luenberger observer (ELO) and extended Kalman filter (EKF) are used to estimate flux components without resorting to the use of intrusive speed sensors. The aim of this paper is to make a comparison and a classification between these approaches. Experimental results demonstrate the significant potential of these methods in detecting these types of faults.

1 INTRODUCTION

Rotor asymmetries in induction machines, for example as a result of broken rotor bars, lead to perturbations in air gap patterns and electromagnetic torque. Over the last twenty years various monitoring and diagnostic strategies have been proposed for the diagnosis of problems in induction motors. These strategies are usually based on the spectral analysis of electrical signatures such as stator currents (Kliman 1992), partial powers (Stanislaw,1996), Park's vector modulus (Cardoso, 1993), (Cruz, 2000) or the electromagnetic torque (Kral, 2000), (Trzynadlowski, 2000), (EL Tabach, 2002). Direct measurement of magnetic field using search coils or Hall-effect sensors means implanting sensors in the air gap of the machine, which leads to increased complexity. Moreover, these sensors are prone to errors caused by temperature variation, noise, etc (Janson, 1992). In order to elaborate only non-invasive diagnostic methods, the electromagnetic torque (EMT) is estimated using internal diagnostic methods. These methods use electrical parameters and a model of the machine in order to estimate state components such as stator or rotor flux, or the electromagnetic torque (EMT). The estimation of these state components requires the measurement of all the three currents and voltages which will be much expensive than the simple current spectrum techniques. However, if implemented in a Variable Frequency Drive "VFD" where current and voltage measurement are already taken, the incremental cost is limited and these drives will provide accurate systems for mechanical faults detection and diagnosis. Some writers like in (Trzynadlowski, 1999) and (Kral, 2000) study the spectral analysis of the electromagnetic torque (EMT) computed from estimations of stator flux and measurements of stator current. This method involves estimating the stator flux without any correction step, which means that the accuracy of flux estimation is low. Others, like Eltabach (EL Tabach, 2002), have proposed analyses of the EMT deduced from the observed rotor flux using linear observers as the Luenberger Observer, and Kalman filtering.

This article widen the idea in (Eltabach, 2002), in fact first, this article treats a new approach using a sliding mode observer applied to the complete order model of induction machines, without sensing or estimation of speed. This design strategy considers

the non-linear induction motor dynamic system as a linear system subjected to bounded uncertainties due mainly to variations in both speed and stator resistance. This offers a number of advantages including simplicity, parameter-insensitivity, and noise rejection. Secondly this article aims to make a comparison and a classification between this new approach and the previous work concerning the EMT estimation methods.

In this paper, section 2 reviews the complete linear model, the complete motor model extended to the velocity and the resistive torque, the sliding mode observer structure, the Luenberger observer and finally the Kalman filtering. Experimental results and a comparison of the detection approaches, for detecting one and two broken bars at three load levels, are presented in section 3.

2 THEORETICAL BACKGROUND

The electromagnetic torque of an induction motor can be computed from certain known motor variables such as stator currents and rotor flux, or stator currents and stator flux. Stator flux can be computed from model-based observers such as the sliding mode observer and the Luenberger observer as a deterministic variable structure approach, and the Kalman filter as a stochastic approach. In this paper we shall deal with both these approaches using the fourth-order model of the induction motor, without resorting to the use of intrusive speed sensors physically integrated into the machine.

2.1 Fourth-order induction motor model

The fourth-order model is obtained by considering the stator voltages as input and the stator currents as output. The state vector consists of the currents and stator flux components. This model is deduced from a Park transformation and presented in a *d-q* plane rotating at velocity w_x. With these assumptions, and assuming the mechanical velocity is known, the linear fourth-order model of the machine can be obtained:

$$\begin{cases} \dot{X}_4 = A_4 X_4 + B_4 U_4 \\ y = C_4 X_4 \end{cases} \quad (1)$$

With

$$X_4 = \begin{bmatrix} I_{sd} \ I_{sq} \ \Phi_{sd} \ \Phi_{sq} \end{bmatrix}^T, U = \begin{bmatrix} V_{sd} V_{sq} \end{bmatrix}^T,$$

$$y = \begin{bmatrix} I_{sd} \ I_{sq} \end{bmatrix}^T$$

$$A_4 = \begin{bmatrix} -\dfrac{(R_s L_r + R_r L_s)}{\sigma L_s L_r} & -(w_m - w_x) & \dfrac{R_r}{\sigma L_s L_r} & \dfrac{w_m}{\sigma L_s} \\ w_m - w_x & -\dfrac{(R_s L_r + R_r L_s)}{\sigma L_s L_r} & -\dfrac{w_m}{\sigma L_s} & \dfrac{R_r}{\sigma L_s L_r} \\ -R_s & 0 & 0 & w_x \\ 0 & -R_s & -w_x & 0 \end{bmatrix} \quad (2)$$

$$B_4 = \begin{bmatrix} \dfrac{1}{\sigma L_s} & 0 & 1 & 0 \\ 0 & \dfrac{1}{\sigma L_s} & 0 & 1 \end{bmatrix}^T, \ C_4 = \begin{bmatrix} 1 & 0 & 0 & 0 \\ 0 & 1 & 0 & 0 \end{bmatrix},$$

$$w_m = P\Omega_m, \ \sigma = 1 - \dfrac{L_r}{L_S} \quad (3)$$

R_s, R_r, L_{fs}, L_r P, Ω_m are respectively the stator resistance, rotor resistance, total leakage inductance, rotor inductance, number of pole pairs, and mechanical velocity.

If the uncertain parameters are split into two parts, the first corresponding to nominal operation and the second to unknown behaviour, the system model (1) can be restated as follows:

$$\begin{cases} \dot{X}_4 = \overline{A}_4 X_4 + \overline{B}_4 U + \Delta A(t).X_4 + \Delta B(t).U \\ y = C_4 X_4 \end{cases} \quad (4)$$

$\overline{A}_4$ and $\overline{B}_4$ are respectively the nominal state and input matrixes, which are assumed to be known. $\Delta A(t)$ and $\Delta B(t)$ represent the uncertainties on A_4 and B_4 due to unmodeled behaviour or parameter drift.

2.2 Extended non-linear induction motor model

To obtain a complete extended model for stator flux and mechanical velocity we consider as in (1) the stator voltages as input $U = [V_{sd} V_{sq}]^T$ and the stator currents as output $y = [I_{sd} I_{sq}]^T$. While the state vector (ζ) consists of the stator current components, stator flux components, mechanical velocity, and finally the resistive torque: $\zeta = [I_{sd} \ I_{sq} \ \Phi_{sd} \ \Phi_{sq} \ w_m \ C_r]^T$. With these assumptions, we obtain non-linear extended motor model:

$$\begin{cases} \dot{\zeta} = f(\zeta) + g(\zeta).U \\ y = h(\zeta) \end{cases} \quad (5)$$

where

$$f(\zeta) = \begin{bmatrix} b\zeta_1 - (P\zeta_5 - w_x)\zeta_2 - a_1\zeta_3 - a_2\zeta_4\zeta_5 \\ (P\zeta_5 - w_x)\zeta_1 + b\zeta_2 + a_2\zeta_3\zeta_5 - a_1\zeta_4 \\ -a_6\zeta_1 + w_x\zeta_4 \\ -a_6\zeta_2 - w_x\zeta_3 \\ a_3\zeta_2\zeta_3 - a_3\zeta_1\zeta_4 - a_4\zeta_6 - a_5\zeta_5 \\ 0 \end{bmatrix}$$

$$a = \frac{1}{L_r^2 - L_r L_s}, b = a.(R_s L_r + R_r L_s), a_1 = a.R_r$$

$$a_2 = aL_r P, a_3 = \frac{3}{2.J_0}, a_4 = \frac{1}{J_0}, a_5 = 0 ,$$

$$g(\zeta) = \begin{bmatrix} \frac{1}{L_{fs}} & 0 & 1 & 0 & 0 & 0 \\ 0 & \frac{1}{L_{fs}} & 0 & 1 & 0 & 0 \end{bmatrix}, h(\zeta) = \begin{bmatrix} \zeta_1 \\ \zeta_2 \end{bmatrix} \quad (6)$$

2.3 Sliding mode observer structure

The principal objective of a sliding mode observer (SMO) structure is to force the observation error to converge to zero by tracking the system output variable, which in our case corresponds to the two stator current components (see Figure 1). In other words, the idea is to track the stator current components by putting the corresponding current errors into sliding mode, hence ensuring the asymptotic convergence of the flux observation errors, despite the stator resistance and the mechanical velocity variations. The observer is based on the nominal part of the rearranged stator flux model, with stator current and voltage measurements as inputs. The system model is then split into two coupled subsystems: the first corresponding to the measurable stator currents, and the second to the stator flux components to be reconstructed. The proposed SMO has the following structure:

$$\dot{\hat{X}}_{4,1} = \overline{A}_{11} y + \overline{A}_{12} \hat{X}_{4,2} + \overline{B}_1 U + K_1 \text{sgn}(s) \quad (7)$$

$$\dot{\hat{X}}_{4,2} = \overline{A}_{21} y + \overline{A}_{22} \hat{X}_{4,2} + \overline{B}_2 U + K_2 \text{sgn}(s)$$

where ($y = \hat{X}_{4,1}$) and $\hat{X}_{4,2}$ are the estimated stator current and flux components respectively:

$$\hat{X}_{4,1} = [\hat{i}_{ds} \ \hat{i}_{qs}]^t, \ \hat{X}_{4,2} = [\hat{\phi}_{ds} \ \hat{\phi}_{qs}]^t \quad (8)$$

$$\overline{A}_4 = \begin{bmatrix} \overline{A}_{11} & \overline{A}_{12} \\ \overline{A}_{21} & \overline{A}_{22} \end{bmatrix}, \overline{B}_4 = \begin{bmatrix} \overline{B}_1 \\ \overline{B}_2 \end{bmatrix}, \overline{A}_{22} = 0, \overline{B}_2 = I_2 \quad (9)$$

The vector "s" is the stator currents subsystem switching function. It is directly related to the stator currents observation error. "K_1" and "K_2" are gain matrixes to be designed. For more details on the gain

design procedure, one can refer to (Kheloui., 2000).

2.4 Luenberger observer

The deterministic discrete time model of the machine is deduced from system (5) by discrimination to the first-order approximation:

$$\begin{cases} \zeta_{k+1} = \zeta_k + T_e \dot{\zeta}_k = f_d(\zeta_k, U_k) \\ Y_k = h(\zeta_k) = C_k . \zeta_k \end{cases} \quad (10)$$

Indices k and $k+1$ refer to the variable values at "t_k" and "t_{k+1}" respectively. "T_e" denotes the sampling period in milliseconds. Before applying the Luenberger estimation procedure, the nonlinear model (10) must be linearized. The linearization of this non linear model is given by (11) by calculating the following Jacobians (12):

$$\begin{cases} \zeta_{k+1} = f_d(\zeta_k, U_k) = \hat{A}_k \zeta_k + \hat{B}_k U_k \\ Y_k = h(\zeta_k) + V_k = C_k . \zeta_k \end{cases} \quad (11)$$

$$\hat{A}_k = \frac{\partial f_d}{\partial \varsigma}\bigg|_{\varsigma_k = \hat{\varsigma}_k} \quad \hat{B}_k = \frac{\partial f_d}{\partial U}\bigg|_{\varsigma_k = \hat{\varsigma}_k} \quad C_k = \frac{\partial h}{\partial \varsigma}\bigg|_{\varsigma_k = \hat{\varsigma}_k} \quad (12)$$

The Luenberger state vector estimation method consists of two phases. First, the state is predicted according to the model given in (13).

$$\begin{cases} \hat{\varsigma}_{k+1/k} = f_d(\hat{\varsigma}_{k/k}) \\ \hat{Y}_{k+1/k} = h(\hat{\varsigma}_{k/k}) \end{cases} \quad (13)$$

Then the predicted state vector is corrected by injecting the output estimation error:

$$\hat{\varsigma}_{k+1/k+1} = \hat{\varsigma}_{k+1/k} + K_{luenb}(Y_{k+1} - \hat{Y}_{k+1/k}) \quad (14)$$

The gain "K_{luenb}" is calculated by pole placement using the command "PLACE" from "MATLAB".

2.5 Kalman Filter

The stochastic discrete time model of the machine is deduced from system (5) by discrimination to the first-order approximation, taking state and measurement noises into account:

$$\begin{cases} \zeta_{k+1} = \zeta_k + T_e \dot{\zeta}_k + W_w = f_d(\zeta_k, U_k) + W_k \\ Y_k = h(\zeta_k) + V_k = C_k . \zeta_k + V_k \end{cases} \quad (15)$$

$$Q_k = E\{W_k W_k^t\}, \ R_k = E\{V_k V_k^t\} \quad (16)$$

"W_k" and "V_k" are the state and measurement noises respectively. We suppose that these noises are white, Gaussian and zero-mean. These noises are defined by their covariance matrices (Q_k, R_k). For simplicity, they are taken to be diagonal matrices. Before applying the Kalman filter procedure, the nonlinear

model (15) must be linearized (17) as in the Luenberger observer procedure (19):

$$\begin{cases} \zeta_{k+1} = f_d(\zeta_k, U_k) = \hat{A}_k \zeta_k + \hat{B}_k U_k + W_k \\ Y_k = h(\zeta_k) + V_k = C_k.\zeta_k + V_k \end{cases} \quad (17)$$

$$\hat{A}_k = \frac{\partial f_d}{\partial \zeta}\bigg|_{\zeta_k = \hat{\zeta}_k} \quad \hat{B}_k = \frac{\partial f_d}{\partial U}\bigg|_{\zeta_k = \hat{\zeta}_k} \quad C_k = \frac{\partial h}{\partial \zeta}\bigg|_{\zeta_k = \hat{\zeta}_k} \quad (18)$$

The KF consists of two phases. First, the state is predicted according to the model given in (19).

$$\begin{cases} \hat{\zeta}_{k+1/k} = f_d(\hat{\zeta}_{k/k}) \\ \hat{Y}_{k+1/k} = h(\hat{\zeta}_{k/k}) \end{cases} \quad (19)$$

Subsequently, this prediction is corrected by injecting the output estimation error:

$$\hat{\zeta}_{k+1/k+1} = \hat{\zeta}_{k+1/k} + K_{k+1}(Y_{k+1} - \hat{Y}_{k+1/k}) \quad (20)$$

Indices *(k+1)/k* and *(k+1)/k+1* means respectively the estimated and the corrected value at t_{k+1}. For more details on this estimator see (Eltabach, 2002). Finally, the Open Loop method of the state estimation consists only of the first phase of the Kalman filter, that is to say without any correction of the state.

3 EXPERIMENTAL SETUP

The experimental tests were carried out using data from the University of Poitiers (France) downloadable from http://laii.univ-poitiers.fr/. The equipment used:

1- Motor: 220/380 V; 50 Hz; 1.1 kW; P=2.

2- Electrical parameters of the motor: R_s=11 Ω, R_r=3.75 Ω, L_{fs}=0.04H, L_r=0.47 H

3- Three voltage sensors
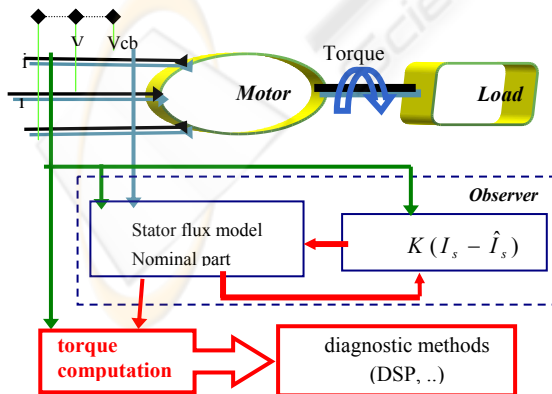
Figure 1: Experimental setup

4- Three current sensors

5- An incremental position sensor (2048-point).

The measured signal-sampling period was 0.7 ms. The detection tests were performed with the equipment described above, first using an undamaged motor, subsequently motor with one and finally two broken bars. In each case three different levels of load full, medium and low were used, corresponding to 100%, 60% and 22% of the nominal torque respectively.

3.1 Electromagnetic torque spectral analysis

The spectrum of the instantaneous electromagnetic torque contains a signature related to the mechanical fault. In fact, broken rotor bars give rise in the torque's spectrum to a component of frequency "*2sf*", "*f*" being the fundamental frequency and "*s*" the slip.

The electromagnetic torque can be obtained by multiplying stator flux and stator currents. In order to avoid measuring stator flux, the components of the stator flux can be estimated by approaches including Kalman filtering and observers. An estimated torque can be computed from the following equation:

$$C_{em} = \frac{3}{2}P\left(\hat{\Phi}_{sd} I_{sq} - \hat{\Phi}_{sq} I_{sd}\right) \quad (21)$$

where $\hat{\phi}_{sd}, \hat{\phi}_{sq}$ are the estimated stator flux components.

Figures (2a, 2b, 2c) show the normalized spectrum (in dB) with respect to its mean value, computed from the stator currents and estimated stator flux using the extended Kalman filter estimation method at three different load levels. Figures (3a, 3b, 3c) show the normalized spectrum computed from the estimation of stator flux using the sliding mode observer. The experimental results for EKF, ELO and SMO clearly reveal the existence of spectral peaks at a fault characteristic frequency "*2sf*" when broken bars are present. When two bars are broken this frequency takes the value of 4.5 Hz, 2.7 Hz, 0.6 Hz for full, medium, and low load levels respectively. In the presence of just one broken bar the corresponding values are 4.2 Hz, 2.2 Hz, 0.5 Hz. Notice that the amplitude of the fault characteristic frequency "*2sf*" is directly linked to the severity of the fault. In other words, this amplitude for all three load levels is more pronounced in the case of two broken bars than when there is just one broken bar.
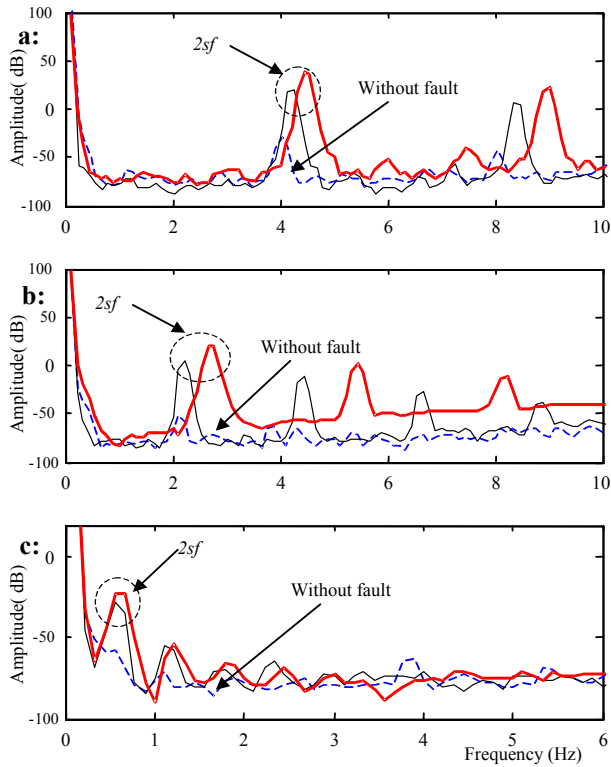
Figure 2: Torque spectrum calculated from stator flux using EKF (thick line: two broken bars, thin line: one broken bar, dashed: fault-free) for load levels: a. Full, b. Medium, c. Low
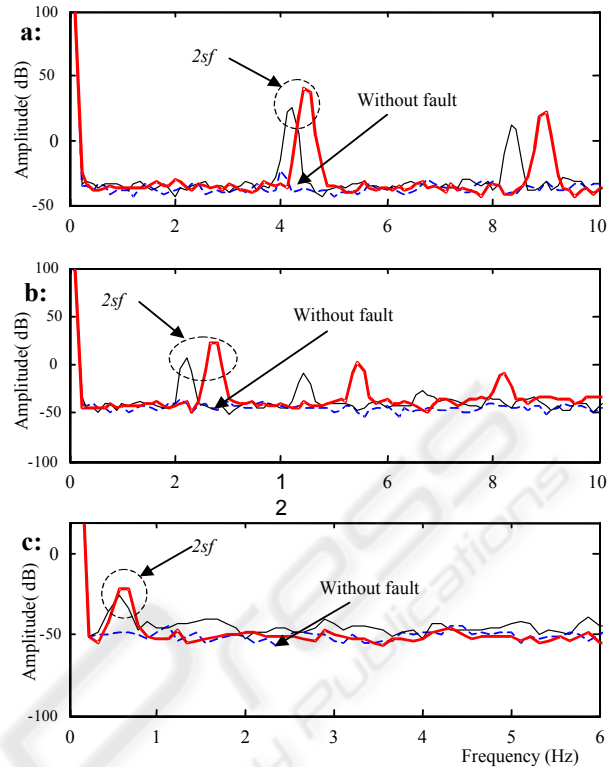
Figure 3: Torque spectrum calculated from stator flux using SMO (thick line: two broken bars, thin line: one broken bar, dashed: fault-free) for load levels: a. Full, b. Medium, c. Low
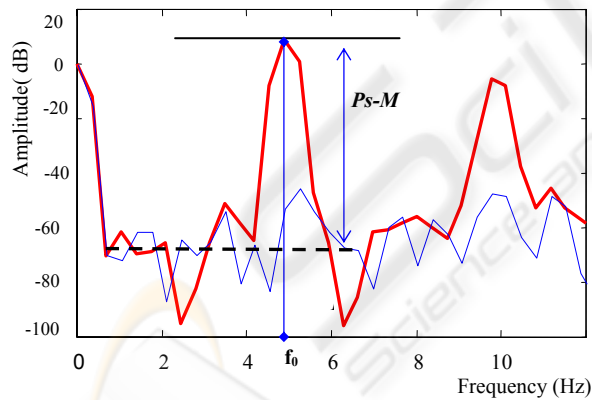
Figure 4: Comparison criterion
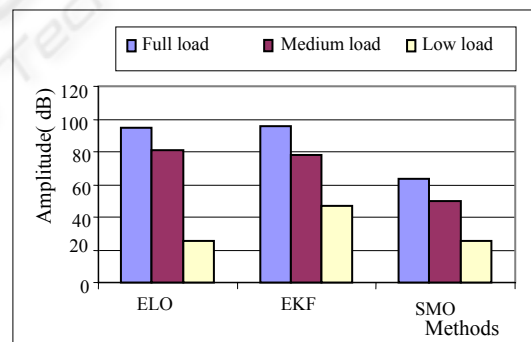
Figure 5: Comparison criterion values « R » at three load levels in case of one broken bar, and function of the estimation method.
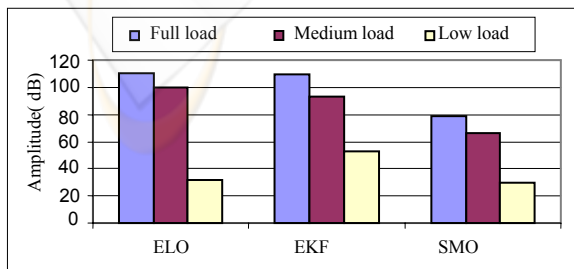
Figure 6: Comparison criterion values « R » at three load levels in case of two broken bar, and function of the estimation method.

3.2 Comparison

The spectral analysis of the estimated electromagnetic torque computed by different methods clearly shows that when a rotor fault is present a component appears at the fault's characteristic frequency « $f_0 = 2sf$ » and his amplitude is directly linked to the severity of the fault. In order to elaborate motor mechanical diagnosis, a criterion "R" is used to represent the severity of the mechanical fault see Figure 4.

$$R = P_S - M \quad \text{in dB} \tag{22}$$

"P_s" is the amplitude of the fault characteristic frequency. "M" is the spectrum average, for a fault-free motor, in the range where the fault characteristic frequency may occur. In our case the range is [0.3 Hz, 5 Hz], corresponding to the fault characteristic frequency at no load and at 120% of the motor nominal load. Figure 5 and Figure 6 show a comparison between all the three diagnosis methods with respect to the comparison criterion "R", at three load levels in case of one Figure 5 and two broken bars Figure 6. Experimental results clearly show that the EKF and ELO methods are better able than the SMO observer to detect broken bars at all load levels. EKF and ELO detection methods were comparable as regards their capacity to detect mechanical faults, although EKF displayed a much higher comparison criterion at low load levels.

4 CONCLUSION

This paper has treated a new detection approach using a sliding mode observer and compared three non-invasive approaches for the detection of rotor imperfections. In a first approach, the sliding mode observer (SMO) is used to estimate stator flux components in the absence of any speed sensing or speed estimation. The second approach uses an extended Kalman filter (EKF) and the third approach uses an extended Luenberger observer for flux components and velocity estimation. Experimental results using real electrical signals (assuming no change in motor parameters) show the importance of using the Kalman filter to estimate the electromagnetic torque, which can provide more effective detection of rotor faults even at low load levels. We are currently concentrating on the sensitivity of these two approaches to natural variations in electrical parameters, which can sometimes give rise to false alarms.

REFERENCES

Cardoso, A.J.M., 1993. Computer-Aided Detection of Airgap eccentricity in operating three phase induction's Motors by park vector Approach. In *IEEE Transactions on Industry Applications*, vol. 29 N° 5, pp. 897–901.

Cruz, S.M.A et al., 2000. Rotor cage Fault Diagnosis in three-phase induction Motors by Extended Park's Vector Approach. In *Electric Machines and Power Systems*, vol. 28, pp.289-299.

El tabach, M., 2002. Detection of induction motors broken bars by electromagnetic torque estimation using Kalman filtering. In *EPE-PEMC, 10th International Power Electronics and Motion Control conference*, Dubrovnik, Croatia.

Janson, 1992. A physically insightful approach to the design and accuracy assessment of flux observers for field oriented induction machine drives. In *IEEE – IAS Annual meeting record*, pp. 570-577.

Kheloui, A., 2000. Design of a stator flux sliding mode observer for direct Torque control of Sensorless induction machine. In *IEEE Industry Application Conference*, vol. 3, pp.1388-1393

Kliman, G.B., 1992. Methods of motor current signature Analysis. *In Electric Machines and Power Systems*. Vol. 20 N° 5 , pp. 463-474.

Kral, Ch., et al., 2000. Sequences of field-oriented Control for the detection of faulty rotor Bars in induction Machines, the Vienna monitoring method. In IEEE Transactions on Industrial Electronics, vol. 47 N° 5, pp. 1042-1050.

Stanislaw, F. et al., 1996. Instantaneous Power as a medium for the signature analysis of induction Motors. In *IEEE Transactions on Industry Applications*, vol 32 N° 4, pp. 904-909.

Trzynadlowski, A.M et al., 2000. Comparative Investigation of Diagnostic Media for Induction Motors: a case of rotor cage faults. In *IEEE Transactions on Industrial Electronics*, vol. 47, pp. 1092 –1099.